Preparation and Properties of Polythiourethane/ZnS Nanocomposites with High Refractive Index

Li Liu,[1,2] Zhen Zheng,[1,2] Xinling Wang[1,2]

[1]*School of Chemistry and Chemical Engineering, Shanghai Jiao Tong University, Shanghai 200240, People's Republic of China*
[2]*State Key Laboratory of Metal Matrix Composites, Shanghai Jiao Tong University, Shanghai 200240, People's Republic of China*

Received 2 November 2009; accepted 27 December 2009
DOI 10.1002/app.32009
Published online 5 April 2010 in Wiley InterScience (www.interscience.wiley.com).

ABSTRACT: The inorganic–organic crosslinking polythiourethane/ZnS (PTU/ZnS) nanocomposites with high refractive index and transmittance were successfully prepared. The thiol-capped ZnS nanoparticles with a diameter of about 5 nm were fabricated into the molecular chains of PTU via the formed covalent bonds between the capped ZnS and the matrix. The investigations demonstrated the ZnS nanoparticles were uniformly dispersed in the PTU matrix even at high contents. The optical studies showed the refractive index of the highly transparent nanocomposite films linearly increased from 1.643 to 1.792 with the increase of the ZnS content. The structure, morphology, and other properties were also characterized by FTIR, NMR, AFM, XRD, DSC, TGA, etc. © 2010 Wiley Periodicals, Inc. J Appl Polym Sci 117: 1978–1983, 2010

Key words: nanocomposites; polyurethanes; refractive index; nanocomposite; ZnS; polyurethane

INTRODUCTION

Recently, the high refractive index optical materials have attracted wide interest for their potential applications in lenses, special adhesives, and coatings, antireflection films.[1–3] However, traditional organic optical materials are facing great challenge for their relatively low refractive index ($n < 1.6$ at 630 nm) and poor thermal stability. One of the most effective methods to prepare high refractive index nanocomposites is introducing inorganic particles such as ZnS, CdS, PbS with high refractive index ($n > 2.0$ at 630 nm) into bulk organic polymers. In recent years, different organic/inorganic optical nanocomposites with high refractive index have been reported.[4–6] Li[7] prepared the highly transparent epoxy/TiO_2-SiO_2 nanocomposites through introduction of the core-shell structured nanoparticles into epoxy resin. Wu[8] synthesized several kinds of high-refractive-index polymer/TiO_2 nanocomposites with sol–gel method. Lue[9] prepared a series of organic polymer/ZnS nanocomposites with high refractive index, such as the DMAA-St-DVB/ZnS nanocomposites by γ-ray irradiation initiated bulk polymerization, the PUMM/ZnS nanocomposites by UV curing polymerization,[10] and the PTU/ZnS nanocomposites by introducing PhSH/ME-capped ZnS nanoparticles to the linear PTU oligomer, which was prepared with 2,2′-dimercaptoethylsulfide (MES) and isophorone diisocyanate (IPDI).[11]

Generally, there are two crucial drawbacks in preparing the high-refractive-index organic/inorganic nanocomposites with high content of inorganic nanoparticles.

One is the fragility of organic/inorganic hybrid materials due to the rigid character of inorganic nanoparticles. Thereby, it is important to select the appropriate flexible polymers with high refractive index as the matrices. Nicol et al.[12] indicated that the molecular chain of poly(propylene sulfide) (PPS) was flexible for the weak hydrogen bond in polymer. The flexibility of polymer was advantageous for inorganic nanoparticles to be fabricated into organic/inorganic nanocomposites.[12] Furthermore, according to the Loentz-loren theory,[13] the nearly colorless transparent aliphatic sulfur-containing polymer has higher refractive index, which makes the sulfur-contained PPS the appropriate matrix for optical materials with high refractive index. Another drawback is that nanoparticles are prone to aggregation in polymer for their large specific surface area; in addition, the diameter of the inorganic particles in optical polymers should be less than one-tenth of the wavelength of visible light to avoid Rayleigh scattering.

In this article, we tried to directly immobilize the thiol-capped ZnS nanoparticles to the molecular

Correspondence to: X. Wang (xlwang@sjtu.edu.cn).

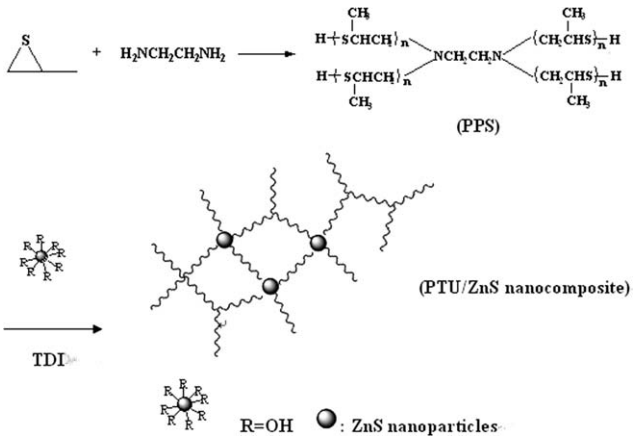

Scheme 1

chains of PTU to synthesize the organic–inorganic cross-linking polythiourethane/ZnS (PTU/ZnS) nanocomposites. Firstly, a branched polypropylene sulfide (PPS) was synthesized as shown in scheme 1, and then, the thiol-capped ZnS nanoparticles and PPS were bonded together through the NCO active groups of TDI. The cross-linking PTU /ZnS nanocomposites were formed via the reactions between isocyanate groups and both the hydroxyl groups on the surface of ZnS nanoparticles and the mercapto groups in PPS. With the branched structure of PPS and multigroups in the molecular chains, more of the capped ZnS nanoparticles were bonded in the molecular chains of PTU than that in linear PTU for per molecular unit, it was benefit for more of the capped ZnS nanoparticles to be introduced or dispersed into the netty structure of PTU matrix without agglomeration.

EXPERIMENTAL

Materials

Propylene sulfide (TCI Chemical Ltd.Com.), toluene diisocyanate (TDI, Mitsui Chemicals.), ethylenediamine, zinc acetate dehydrate, 2-mercaptoethanol (ME) (TCI Chemicals Co.), thiourea, *N*,*N*′-dimethylformamide (DMF), 3,3′-dichloro-4,4′-di aminodiphenylmethane (MOCA) (TCI Chemicals Co.), dimethyl sulphoxide (DMSO), all of these aforementioned solvents were dried with CaH_2 and purified by vacuum distillation before usage. Besides aforementioned chemicals, all the other chemicals were purchased from Sinopharm Chemical Regent Co. and used as received.

Synthesis of branched poly(propylene sulfide)

The PPS was synthesized according to the modified literature procedure.[14] 15.75 g propylene sulfide, 0.3 g 1,2-ethylenediamine and 10 g DMF were loaded in a 50 mL stainless autoclave and heated at 80°C for 2 h and 130°C for 0.5 h. Then, the mixture was poured into a 200 mL beaker and 40 mL 0.5 mol/L hydrochloric acid was fed into the cooled mixture. After the mixture was stirred for 1 h at room temperature, it was precipitated in methanol and the separated viscous PPS was washed with vast deionized water. The viscous crude PPS was purified by removing the volatile substances at 100°C under reduced pressure. ^{13}C-NMR ($CDCl_3$) δ: 20.95 (C of CH_3 in PPS chain), 38.46 (C of CH_2 in PPS chain), 41.38 (C of CH in PPS chain), 49.3 (C of CH_2 in NCH_2CH), 55.44 (C of CH_2 in CH_2N). The calculated M_n is about 1240.

Synthesis of thiol-capped ZnS nanoparticles (Capped ZnS)

According to the literature procedure,[15] 6.6 mmol Zinc acetate dehydrate, 4.5 mmol thiourea and 13.2 mmol 2-mercaptoethanol were completely dissolved with 150 mL DMF in a three-necked, round bottom flask, the mixture was stirred and refluxed for about 10–12 h under N_2 atmosphere. The refluxed solution was condensed with a rotary evaporator, and the white sediments were precipitated by alcohol. The capped ZnS white powder was purified by filtered, thoroughly washed with methanol and dried in a vacuum oven at 50°C for 12h.

Synthesis of polythiourethane/ZnS (PTU /ZnS) nanocomposites

The calculated weight ratio of PPS and capped ZnS nanoparticles were completely dissolved in DMSO and slowly added into required amount of TDI. After the mixture was vigorously stirred at 60–70°C for about 4 h in N_2 atmosphere, the volatiles in the mixture were removed in a vacuum oven under vacuum to cure the hybrid materials at 60°C for 4 h, 100°C for 2 h, 120°C for 1 h, and 150°C for 0.5 h.

Characterization

FTIR spectra were obtained by a PerkinElmer 1000 FTIR spectrometer. ^{13}C-NMR spectrum was obtained from Mercury plus 400. Samples were dissolved in $CDCl_3$. Thermogarvimetric analysis (TGA) was investigated by a Q5000IR thermal analyzer from 20 to 500°C at heating rate of 20°C/min under N_2 flow. Glass transition temperature was recorded on a TA Q2000 differential scanning calorimeter in N_2 atmosphere at heating rate of 10°C/min from −80 to 120°C. Transmittance was measured with a Tu-1901 spectrophotometer from 400–800 nm. The thickness of all of the samples was about 500 nm. The uncured viscous mixture of PPS, TDI, and capped ZnS was

spin coated on a silicon wafer at 1000–3000 rpm for 10–30 sec. The coated films were cured following the curing procedure of PTU/ZnS nanocomposites. The refractive index at 630 nm was measured by a W-VASE32TM Ellipsometer. The thickness of the samples was between 100–200 nm. The uncured viscous mixture of PPS, TDI, and capped ZnS was spin coated on a silicon wafer at 2000–4000 rpm for 10–30 sec. The coated films were cured following the cured procedure of PTU/ZnS hybrid materials. The size of ZnS nanoparticels was investigated by aJEM-2010 transmission electron microscope. A drop of uncured diluted mixture of PPS, TDI, and capped ZnS was placed on a copper grid and left to cure before transferring into the TEM sample chamber. The wide-angle X-ray diffraction patterns were recorded by a D/max-2200/PC X-ray diffractometer at a scanning rate of 6°/min in 2Θ ranging from 15 to 60° with Cu Kαrasiation (λ = 0.1542). The morphology and phase were investigated by a Veeco-bioscope atomic force microscopy (AFM). The procedure of making samples was same to that for Ellipsometer.

RESULTS AND DISCUSSION

The FTIR spectra of PTU (cured by MOCA), PTU/ZnS nanocomposite and the capped ZnS were presented in Figure 1. As shown in Figure 1(a), the absorption peaks at 3308 cm^{-1}(νN—H), 1650 cm^{-1}(νC=O) and 1446 cm^{-1}(νC—N) were the characteristic absorption peaks of PTU. In Figure 1(c), the absorption peaks at 2916cm^{-1}(νC—H) and 1421 cm^{-1}(νC—H) indicating the existence of the methylene group of ME on ZnS. The peaks at 3421 and 1258 cm^{-1} were assigned to the characteristic peaks of OH in ME. These peaks showed the ZnS nanoparticles had been wrapped by ME. The absorption peak of the S–H vibration at 2550–2565 cm^{-1} was not observed in the IR spectrum, indicating that the mercapto groups of ME molecules were bound to the ZnS nanoparticle surface.[16] In Figure 1(b), the characteristic absorption peaks of C—O bond in ME (1046 cm^{-1}), C=O bond (1650 cm^{-1}) and C—N bond (1446cm^{-1}) in PTU were observed. However, the characteristic peaks of OH on the capped ZnS nanoparticles disappeared and the peak of C=O was broadened. The results suggested OH groups on ZnS nanoparticles reacted with NCO groups, and the capped ZnS nanoparticles were fabricated into the molecular chains of PTU by forming new —NHCO— covalent bonds. In Figure 1(b), the characteristic peak of NH shifted to 3334 cm^{-1}, which might attribute to the hydrogen bonds in the nanocomposites being weakened by ZnS nanoparticles. The weakened intramolecular and intermolecular hydrogen bonds of PTU could probably decrease the hindrance while the capped ZnS nanoparticles were dispersed into the PTU matrix. It would be helpful to prepare the uniform PTU/ZnS nanocomposites.

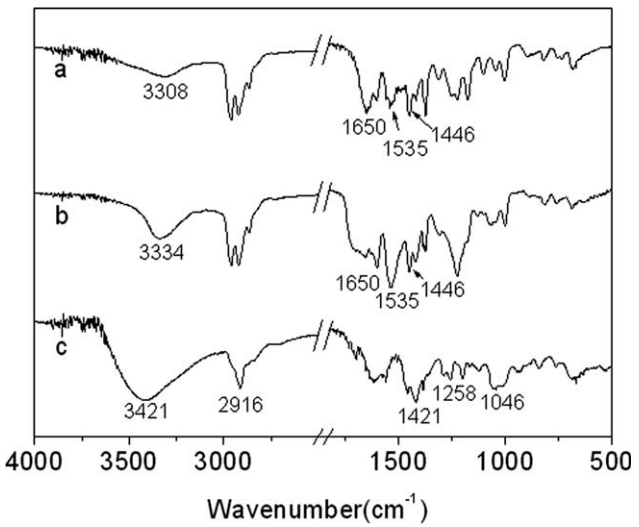

Figure 1 FTIR spectra of PTU cured by MOCA (a), PTU/ZnS nanocomposite with 45 wt % capped ZnS nanoparticles (b), the capped ZnS (c).

Nanoparticles are prone to agglomeration in polymer for their large specific surface area and poor compatibility with polymer. The interactions between nanoparticles and polymers play a crucial role for improving the dispersion of nanoparticles in polymers. TEM images of PTU/ZnS nanocomposites were shown in Figure 2. The capped ZnS nanoparticles were evenly distributed in the worm-like matrix without obvious aggregation. The size of the nanoparticles was about 5 nm, it wouldn't block the diffusion of visible light for it was far less than one-tenth of the wavelength of visible light. Figure 2(a) was the TEM image of polyurethane/ZnS (PU/ZnS) nanocomposite with 20 wt % capped ZnS nanoparticles, it was prepared by simply blending the linear polyurethane and capped ZnS nanoparticles in DMF with ultrasonic for 30 min, there were no covalent interaction between the linear polyurethane and the capped ZnS nanoparticles. The poor dispersion of the capped ZnS nanoparticles in PU was obviously observed (within the cycle marked area in the image) in the PU/ZnS nanocomposite, and it was worse than that in PTU matrix even with lower content of the nanoparticles (20 wt %). For the PTU/ZnS nanocomposite, the capped ZnS nanoparticles were uniformly dispersed in PTU matrix with much higher content (65 wt %) of the ZnS nanoparticles. The contrasting experimental results proved that forming strong interactions between polymer and nanoparticles was one of the effective ways to improve the dispersion of nanoparticles in polymers.

AFM measurements were performed to identify changes on the surface morphology of PTU/ZnS

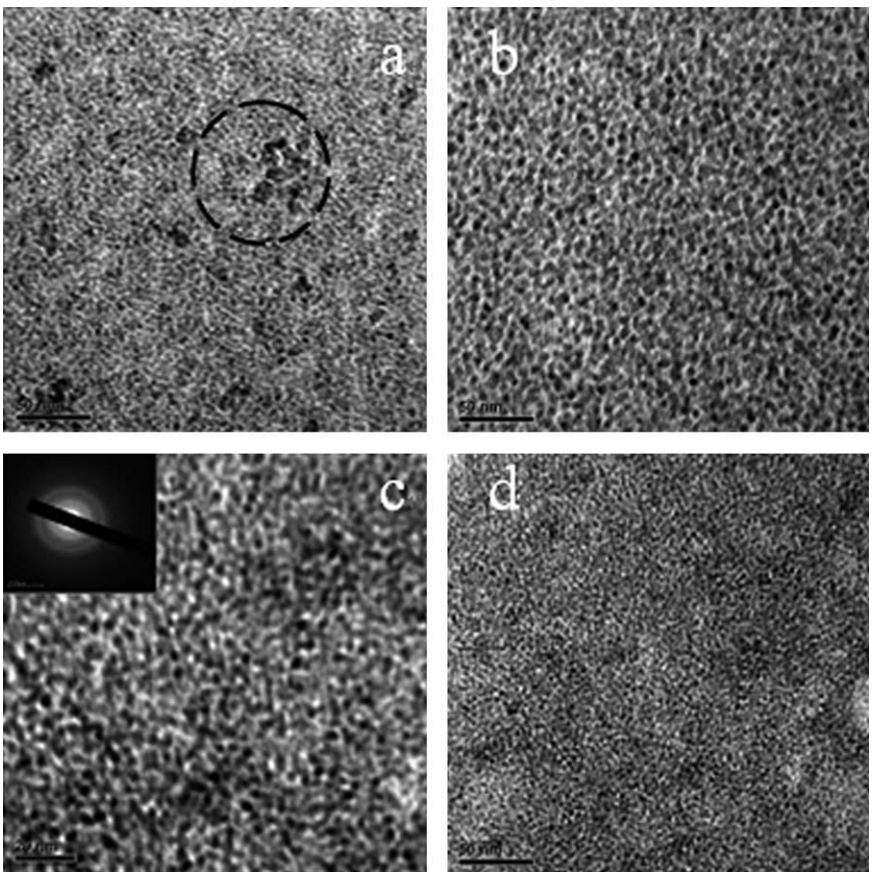

Figure 2 TEM images of linear PU/ZnS nanocomposites with 20 wt % capped ZnS (a), PTU/ZnS nanocomposite with 35 wt % capped ZnS (b), PTU/ZnS nanocomposite with 65 wt % capped ZnS (c) and (d), (the scales are 20 and 50 nm, respectively).

nanocomposites with different contents of ZnS nanoparticles. The PTU/ZnS nanocomposites (Fig. 3) presented two crossed and separated contrasting phase, which was attributed to the phase separation of soft and hard blocks in PTU molecular chains, respectively. The degree of phase separation increased with the increase of the content of ZnS nanoparticles. The reason was that most of the rigid ZnS nanoparticles were immobilized on the hard blocks of PTU and it improved the degree of the phase separation of the hard and soft blocks of PTU. The phase separation hardly affected the transmittance of the nanocomposite films because the size of phase domain was in nanometer scale. In Figure 3, the two

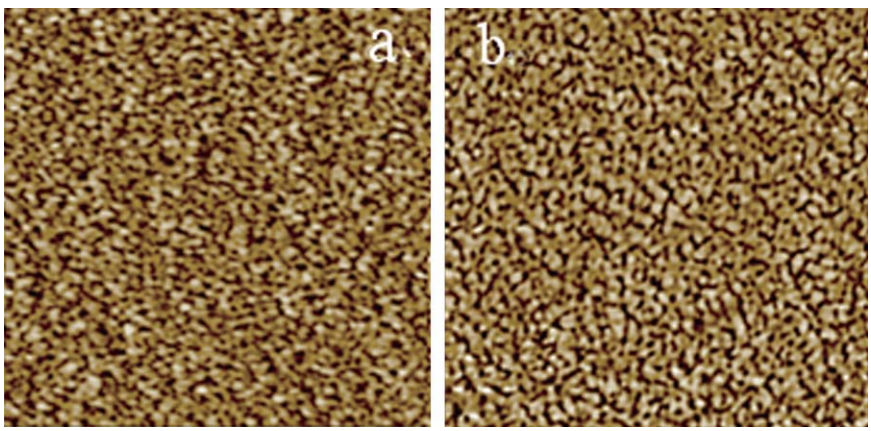

Figure 3 AFM images of PTU/ZnS nanocomposites with 35 wt % capped ZnS (a), with 65 wt % capped ZnS (b). (The scale is 1 μm). [Color figure can be viewed in the online issue, which is available at www.interscience.wiley.com.]

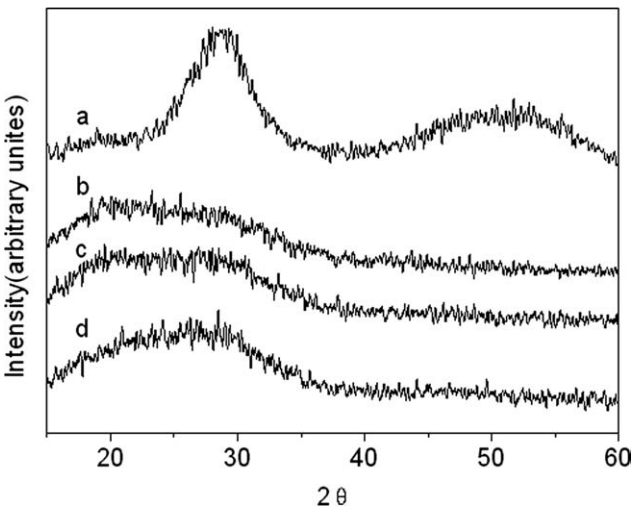

Figure 4 Wide-angle X-ray diffraction patterns of capped ZnS (a), PTU/ZnS nanocomposites with 25 wt % capped ZnS (b), with 45 wt % capped ZnS (c), with 65 wt % capped ZnS (d).

phases tightly crossing one another indicated the capped ZnS nanoparticles were not simply dispersed in PTU matrix, however, they were deeply embedded in the network of PTU.

Figure 4 showed the XRD patterns of the capped ZnS and PTU/ZnS nanocomposites with different contents of the capped ZnS nanoparticles. The diffraction peaks of the capped ZnS corresponding to the (111), (220), and (311), suggested the cubic and hexagonal phases in ZnS crystal structure.[15] But there were no apparently diffraction peaks of the capped ZnS nanoparticles while the content of the capped ZnS nanoparticles in the PTU/ZnS nanocomposites had increased to 65 wt %. The intensities of these diffraction peaks of the nanocomposites were

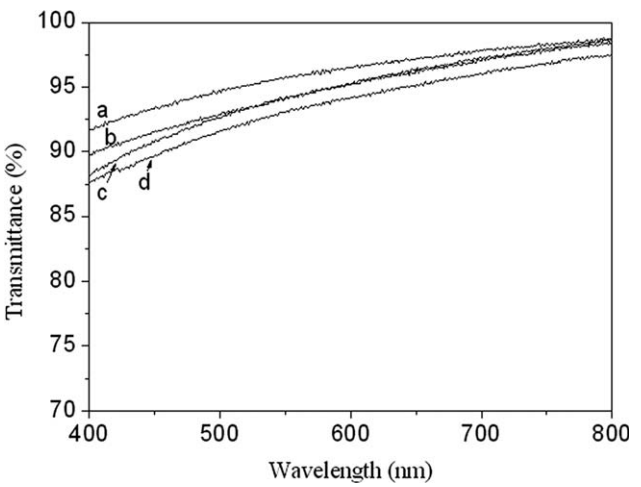

Figure 5 Optical transmittance of PTU (a), PTU/ZnS nanocomposites with 25 wt % capped ZnS (b), with 45 wt % capped ZnS (c), with 85 wt % capped ZnS (d).

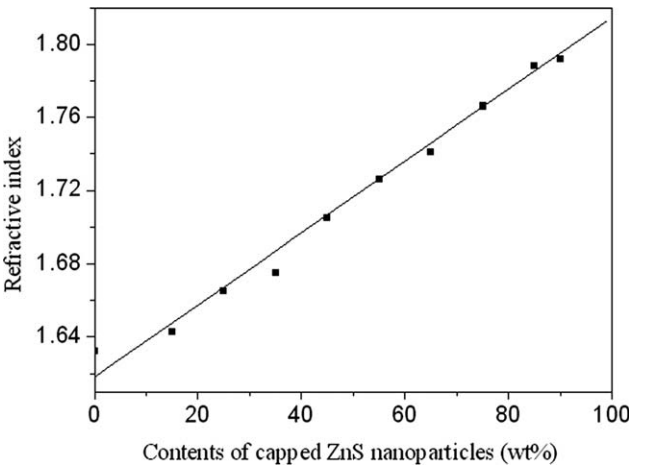

Figure 6 Refractive index (at 630 nm) of PTU/ZnS nanocomposite films with different contents of capped ZnS nanoparticles.

obviously lower than that of pure capped ZnS nanoparticles, and they were lower than that of polymer/ZnS nanocomposite with 40 wt % capped ZnS nanoparticles that were simply dispersed in the polymer without covalent bonds between them.[11] The reason might be most of the capped ZnS nanoparticles in the PTU/ZnS hybrid materials were deeply embedded in the matrix with covalent bonds. It also indicated that the ZnS particles had been successfully fabricated into the PTU matrix.

The investigated results of the optical transmittance and refractive index of the PTU/ZnS nanocomposite films were shown in Figures 5 and 6. The high optical transmittance was one of the most important factors of optical materials. According to the results, the PTU/ZnS nanocomposite films were

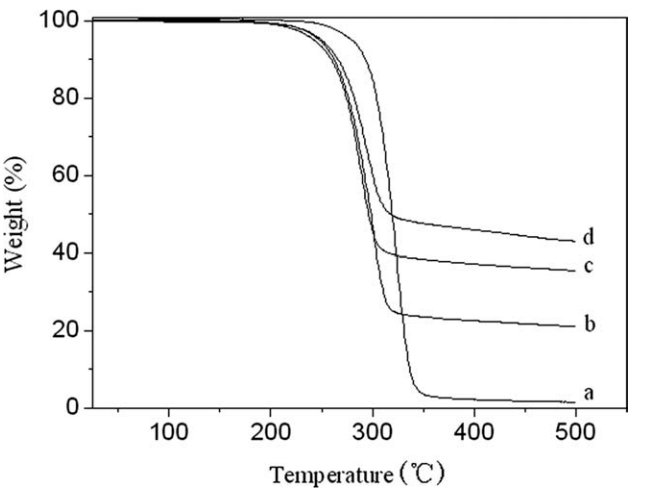

Figure 7 TGA curves of the PTU/ZnS nanocomposites with different contents of capped ZnS nanoparticles. With 0 wt % capped ZnS (a), with 25 wt % capped ZnS (b), with 45 wt % capped ZnS (c), with 65 wt % capped ZnS (d).

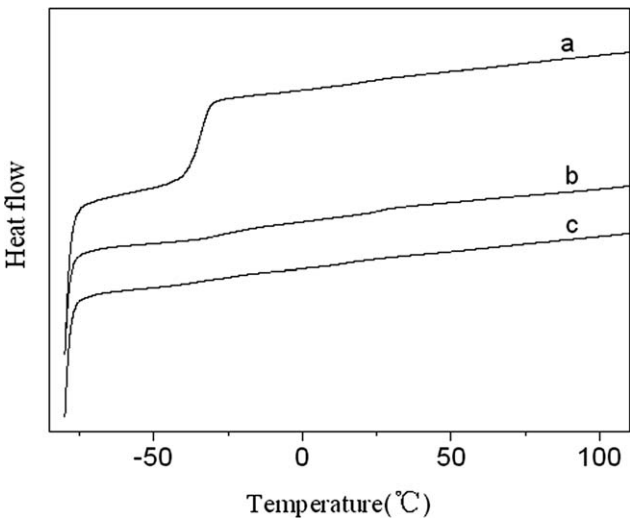

Figure 8 DSC curves of PTU (a), the PTU/ZnS nanocomposites with 45 wt % capped ZnS (b), with 65 wt % capped ZnS (c).

qualified as optical materials as their optical transmittance was higher than 85% in the whole region of visible lightwave. The optical transmittances just decreased by about 5% while the content of the capped ZnS nanoparticles increasing from 0 to 85 wt %. In Figure 6, the refractive index of pure PTU indicated it was feat to be used as optical matrix for its higher refractive index than other polymers. The straight line in Figure 6 showed the refractive index of the nanocomposites linearly increased with the increase of the content of the capped ZnS nanoparticles. The refractive index of the PTU/ZnS nanocomposites increased from 1.643 to 1.792 whereas the content of the capped ZnS nanoparticles increased from 0 to 90 wt %. It proved the ZnS nanoparticles were effective additives to improve the refractive index of PTU. Therefore, the PTU/ZnS nanocomposite films with high transmittance and high refractive index had been successfully prepared.

The thermal properties of PTU and the PTU/ZnS nanocomposites were detected by TGA (Fig. 7). PTU began to decompose at about 293°C, the nanocomposites exhibited a relatively lower initial decomposition temperature due to the thermal decay of ME on the surface of ZnS nanoparticles.[17] For the initial decomposition temperature of the PTU/ZnS, nanocomposite was much higher than the boiling point of pure ME (157°C), it suggested that ME was not simply stacked on the surface of the capped ZnS nanoparticles, presumably, there were complexation between ZnS and ME.

Figure 8 shows the DSC curves of PTU and the PTU/ZnS nanocomposites. The low glass transition temperature (T_g) of PTU (−34°C) indicated the PTU molecular chain was flexible. The height of thermal transition peaks decreased greatly while the content of the capped ZnS nanoparticles increased in the nanocomposites, and there were no obvious thermal transition peaks in curve c. It indicated the crosslinking density and rigidity of the molecular chain were improved by the incorporation of the capped ZnS nanoparticles, which retarded the motion of PTU molecular chains. The nanocomposites became fragile while the content of the ZnS nanoparticles surpassed 65 wt %, but the films with higher concentration of the capped ZnS nanoparticles could still be cast and formed for the flexible PTU matrix.

CONCLUSIONS

The crosslinking polythiourethane/ZnS (PTU/ZnS) nanocomposites with high refractive index and transparency were prepared. The TEM images showed the capped ZnS nanoparticles with an average diameter of 5 nm were uniformly immobilized in PTU with covalent interactions between the ZnS nanoparticles and PTU. The highest refractive index of the nanocomposite films were 1.792 at 630 nm and the transparency of all nanocomposite films was over 85% within the region of visible lightwave. The results indicated that the high refractive index and transparent PTU/ZnS nanocomposites had been successfully prepared with this method. Further work of synthesizing other organic/inorganic composites with this method is underway in our laboratory.

We thank instrumental analysis center of Shanghai Jiao Tong University for the testing support.

References

1. Olshavsky, M.; Allcock, H. R. Macromolecules 1997, 30, 14.
2. Marianucci, E.; Berti, C.; Plati, F.; Manaresi, P.; Guatia, M.; Chiantore, O. Polymer 1994, 35, 7.
3. Sadayori, N.; Hotta, Y. U.S. Pat. 20040158021A1 (2004).
4. Wang, B.; Wilkes, G. L.; Hedrick, J. C.; Liptak, S. C.; Mcgrath, J. E. Macromolecules 1991, 24, 11.
5. Lee, L. H.; Chen, W. C. Chem Mater 2001, 13, 3.
6. Chang, C. C.; Chen, W. C. J Polym Sci Part A: Polym Chem 2001, 39, 19.
7. Li, Y. Q.; Fu, S. Y.; Yang, Y.; Mai, Y. W. Chem Mater 2008, 20, 8.
8. Wu, S.; Zhou, G.; Gu, M. Opt Mater 2007, 29, 12.
9. Lue, C.; Cheng, Y.; Liu, Y.; Yang, B. Adv Mater 2006, 18, 9.
10. Lue, C.; Cui, Z.; Wang, Y.; Yang, B. J Mater Chem 2003, 13, 9.
11. Lue, C.; Cui, Z.; Li, Z.; Yang, B.; Shen, J. J Mater Chem 2003, 13, 3.
12. Nicol, E.; Durand, D.; Nicolai, T. Macromolecules 2001, 34, 1.
13. Solmon, M. Optical Materials: An Introduction to Selection and Application; Marcel Dekker Inc.: New York, 1985; p 10.
14. Cameron, G. M. U.S. Pat. 3,509,112 (1970).
15. Nanda, J.; Sapra, S.; Sarma, D. D. Chem Mater 2000, 12, 4.
16. Hosokawa, H.; Fujiwara, H.; Murakoshi, K.; Wada, Y.; Yanagida, S.; Satoh, M. J Phys Chem 1996, 100, 6649.
17. Chen, S.; Zhu, J.; Shen, Y.; Hu, C.; Li, C. Langmuir 2007, 23, 2.